SMC-TR-95-53

AEROSPACE REPORT NO.
TR-96(8565)-1

Prediction of Stress Relaxation for Compression and Torsion Springs

1 November 1995

Prepared by

D. J. CHANG
Mechanics and Materials Technology Center
Technology Operations

Prepared for

SPACE AND MISSILE SYSTEMS CENTER
AIR FORCE MATERIEL COMMAND
2430 E. El Segundo Boulevard
Los Angeles Air Force Base, CA 90245

Engineering and Technology Group

THE AEROSPACE CORPORATION
El Segundo, California

APPROVED FOR PUBLIC RELEASE;
DISTRIBUTION UNLIMITED

This report was submitted by The Aerospace Corporation, El Segundo, CA 90245-4691, under Contract No. F04701-93-C-0094 with the Space and Missile Systems Center, 2430 E. El Segundo Blvd., Suite 6037, Los Angeles AFB, CA 90245-4687. It was reviewed and approved for The Aerospace Corporation by S. Feuerstein, Principal Director, Mechanics and Materials Technology Center. Capt. Carl L. Kline was the project officer for Mission-Oriented Investigation and Experimentation.

This report has been reviewed by the Public Affairs Office (PAS) and is releasable to the National Technical Information Service (NTIS). At NTIS, it will be available to the general public, including foreign nationals.

This technical report has been reviewed and is approved for publication. Publication of this report does not constitute Air Force approval of the report's findings or conclusions. It is published only for the exchange and stimulation of ideas.

Capt. Carl L. Kline
SMC/SDA

REPORT DOCUMENTATION PAGE

Form Approved
OMB No. 0704-0188

1. AGENCY USE ONLY (*Leave blank*)

2. REPORT DATE
1 November 1995

3. REPORT TYPE AND DATES COVERED

4. TITLE AND SUBTITLE
Prediction of Stress Relaxation for Compression and Torsion Springs

5. FUNDING NUMBERS
F04701-93-C-0094

6. AUTHOR(S)
Chang, Dick J.

7. PERFORMING ORGANIZATION NAME(S) AND ADDRESS(ES)
The Aerospace Corporation
Technology Operations
El Segundo, CA 90245-4691

8. PERFORMING ORGANIZATION REPORT NUMBER
TR-96(8565)-1

9. SPONSORING/MONITORING AGENCY NAME(S) AND ADDRESS(ES)
Space and Missile Systems Center
Air Force Materiel Command
2430 E. El Segundo Blvd.
Los Angeles Air Force Base, CA 90245

10. SPONSORING/MONITORING AGENCY REPORT NUMBER
SMC-TR-95-53

11. SUPPLEMENTARY NOTES

12a. DISTRIBUTION/AVAILABILITY STATEMENT
Approved for public release; distribution unlimited

12b. DISTRIBUTION CODE

13. ABSTRACT (*Maximum 200 words*)

An analytical technique was developed to predict the stress relaxation for compression and torsion springs. The technique uses uniaxial tensile-generated stress-relaxation data for spring wires. Based on the tension-induced stress-relaxation data, the technique was applied to compression springs, where shear stress dominates in predicting the stress relaxation.

This report documents the developed prediction method for stress relaxation of compression and torsion springs and demonstrates the technique using experimental data. When applied to a V-band compression spring made of 302 stainless steel wire, a predicted 2.6% load reduction was obtained after 1000 hr loading as compared with the experimentally measured 2.1% load reduction. Since residual stresses play a significant role over the maximum operating stress range in compression and torsion springs, the calculation method of residual stress is also presented.

14. SUBJECT TERMS
Modeling
Springs
Stress Relaxation

15. NUMBER OF PAGES
27

16. PRICE CODE

17. SECURITY CLASSIFICATION OF REPORT
Unclassified

18. SECURITY CLASSIFICATION OF THIS PAGE
Unclassified

19. SECURITY CLASSIFICATION OF ABSTRACT
Unclassified

20. LIMITATION OF ABSTRACT

NSN 7540-01-280-5500

Standard Form 298 (Rev. 2-89)
Prescribed by ANSI Std. Z39-18
298-102

Contents

Figures

1. Background

Deployable space hardware, such as solar array panels and booms, depends upon spring-stored energy to fulfill its functions. Separation springs at the launch vehicle and payload interfaces need to have nearly identical spring constants that are very accurately calibrated to ensure a load balance during separation. During long-term storage of the satellite, the stored energy of springs in deployable systems may be compromised due to a loss of force in the springs. This loss of force is a direct result of stress relaxation of spring materials. Similarly, the spring forces in separation springs, after an extended period of sitting on the launch pad, may be reduced or become uneven. Both these phenomena can be detrimental to the performance of the satellite or launch operation.

A program has been under way to determine the stress-relaxation behavior of several different high strength alloys that are used in the manufacture of space and satellite springs. These springs use music wire, 302 stainless steel (SS), 17-7 PH SS, Elgiloy, and beryllium-copper (Be-Cu). These materials were procured in wire form and tested using uniaxial tension-type specimens of various lengths. Three levels of test stresses were conducted on the specimens: 0.50, 0.65, and 0.75 F_{tu}, where F_{tu} is the ultimate tensile stress of the spring materials. The tests were conducted in a controlled temperature and humidity environment. The tests generally lasted from 6 weeks (1008 hr) to 12 weeks (2016 hr). The longest test lasted 1 year for 302 SS at both medium and high stress values. The principal investigator for all the experimental work was D. W. Hanna, Structural Materials Department, Mechanics and Materials Technology Center, The Aerospace Corporation.*

Figure 1 depicts a typical stress relaxation curve for 0.05-in.-diam wire made of 302 SS. The vertical ordinate represents the ratio of stress at time t to the initial stress, and the horizontal abscissa represents the time in hours on a log scale. A regression curve fit from the data gives a slope of -0.0116 between the stress ratio and log(t). For higher initial stress, the negative value of the slope increases.

It is of great interest to apply the uniaxially tensile-tested data to springs, in particular, to compression springs in which the stresses are primarily shear. For this objective, a method was worked out to apply the tensile relaxation data to components whose stress state is primarily shear. The details of the application method are described in this report.

*W. D. Hanna, private communication, Structural Materials Department, Mechanics and Materials Technology Center, The Aerospace Corporation, El Segundo, CA.

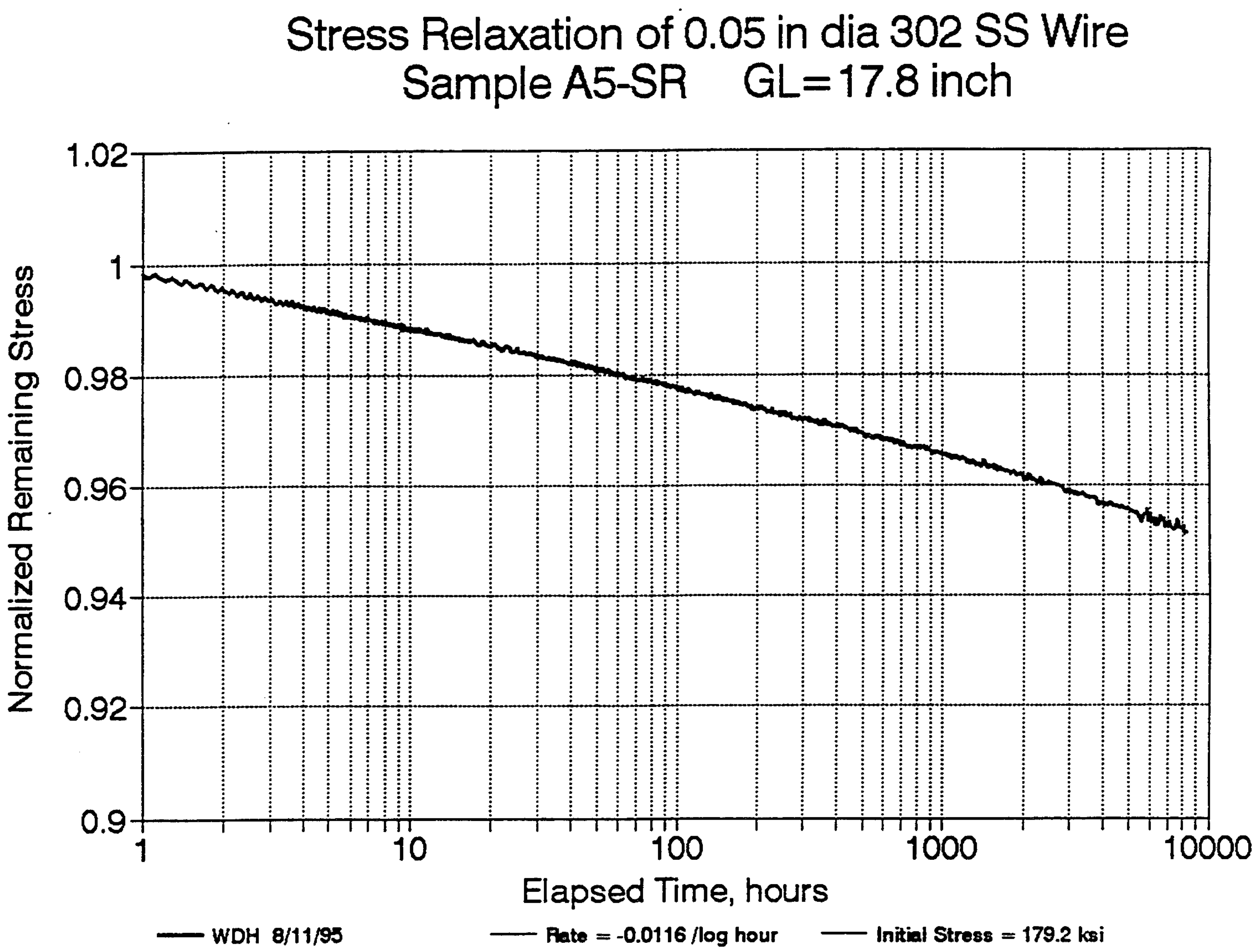

Figure 1. Typical stress relaxation vs time curve for 302 SS wire.

2. Definition of Stress Relaxation

According to the ASTM standards, stress relaxation is defined as "the time-dependent decrease in stress of a solid under given constraint at constant conditions."* The "given constraint" may refer to an initial displacement to induce stresses in the specimen. The "constant conditions" may refer to a constant temperature. From a strain point of view, stress relaxation is a phenomenon where an internal stress existing in a solid body is reduced in magnitude as the elastic strain responsible for the initial stress is partly replaced by plastic strain. When the elastic strain is converted into plastic strain, that part of the strain becomes unrecoverable, and the stress associated with this plastic strain is permanently lost. This loss of the stress constitutes the relaxation of stress.†

* ASTM E-328-86, "Standard Methods for Stress Relaxation Tests for Materials and Structures," *1990 Annual Books of ASTM Standards, Section 3, Metals Test Methods and Analytical Procedures, Vol. 03.01, Metals - Mechanical Testing; Elevated and Low-Temperature Tests; Metallography*, pp. 425-436.

† C. W. Marschall and R. E. Maringer, *Dimensional Instability: An Introduction*, International Series on Materials Science and Technology, Vol. 22, eds. W. S. Owen and D. Eng (Pergamon Press, 1977).

3. Construction of Shear Stress-Strain Curve Based on Uniaxial Tensile Stress-Strain Curve

In attempting to apply the tension stress-relaxation data to shear stressed conditions, it is important to understand the relation between the tensile and shear stress fields. One way to achieve this understanding is to understand the construction of a shear stress-strain curve from a tensile stress-strain curve.

The construction of a shear stress-strain curve using the uniaxial tensile stress-strain curve is based on the following two facts:

1. Plastic strain is solely caused by shear strain.

2. Maximum shear stress is half of the tensile stress in a uniaxial tensile specimen.

For simplicity, it is assumed that the uniaxial stress-strain curve is bilinear. Figure 2a shows this bilinear uniaxial stress-strain curve with stress σ as the vertical ordinate and ε as the horizontal abscissa. The modulus of elasticity is E, and the elastic limit stress and strain are σ_o and ε_o, respectively. The modulus in the inelastic portion of the curve is αE. Similarly, a shear stress-strain curve is constructed as shown in Figure 2b. The vertical and horizontal coordinates are shear stress and strain, τ and γ, respectively, with elastic limit stress and strain τ_o and γ. The shear modulus in the elastic region is G, and that in the inelastic region is ηG. We shall establish the value of η in terms of α and other material constants.

Let us define (σ, ε) and (τ, γ) to be two points on the tensile and shear stress-strain curves, respectively. The slope of the inelastic portion of the tensile curve is

$$(\sigma - \sigma_o) / (\varepsilon - \varepsilon_o) = \alpha E. \qquad (1)$$

Similarly, the slope of the inelastic portion of the shear curve is

$$(\tau - \tau_o) / (\gamma - \gamma_o) = \eta G. \qquad (2)$$

From fact 2, above, we have

$$\tau = \sigma/2, \qquad \tau_o = \sigma_o/2$$

and

• Bi-linear Uniaxial Tensile Stress-Strain Curve

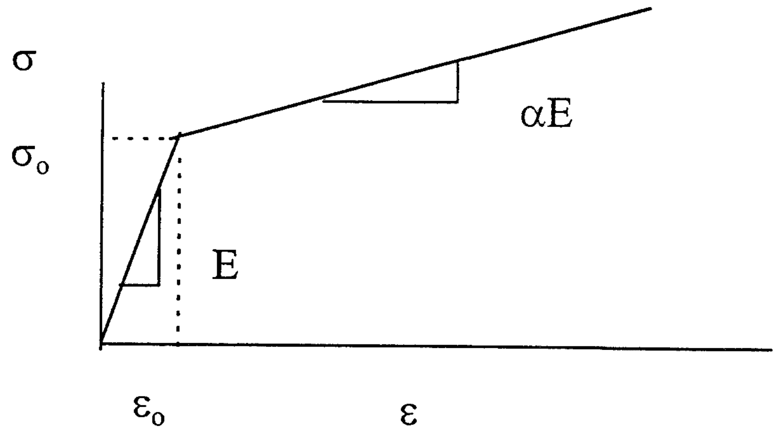

Fig. 2a

• Bi-linear Shear Stress-Strain Curve

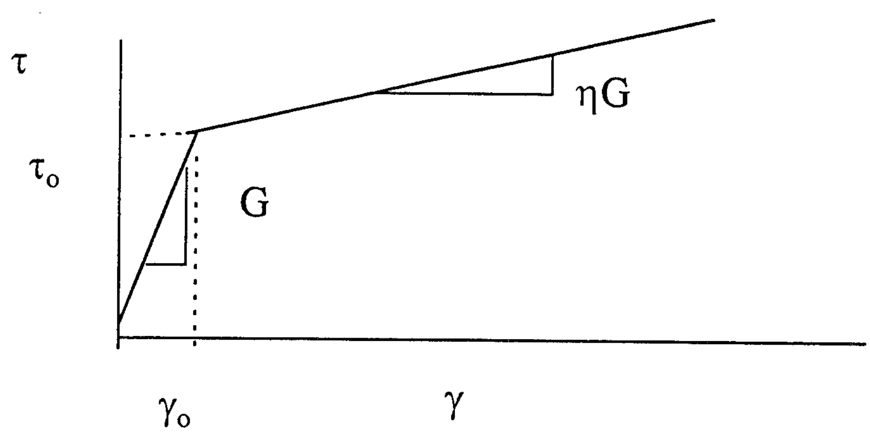

Fig. 2b

Figure 2. Uniaxial and shear bilinear stress-strain curves.

$\gamma = 3\varepsilon/2, \qquad \gamma_o = \tau_o/G.$

Substituting the above relations into Eq. (2), and taking into account the fact that Poisson's ratio in the inelastic region is 1/2, we have

$$(\tau - \tau_o)/(\gamma - \gamma_o) = [(\sigma - \sigma_o)/2]/(3\varepsilon/2 - \tau_o/G) \approx [(\sigma - \sigma_o)/2]/(3\varepsilon/2 - 3\varepsilon_o/2)$$
$$= (\sigma - \sigma_o)/3(\varepsilon - \varepsilon_o) = \alpha E/3.$$

This result and the fact that G = E/3 in the inelastic region give

$$\eta = \alpha. \tag{3}$$

This means that the ratio of the inelastic shear modulus to elastic shear modulus in a shear stress-strain curve is equal to the ratio of the inelastic modulus to elastic Young's modulus in a uniaxial stress-strain curve.

4. Relation Between Tensile and Shear Stress Relaxation

Let $\mathcal{F}(\sigma_o, t, M, T)$ and $\mathcal{b}(\tau_o, t, M, T)$ be the stress-relaxation functions associated with tension and shear modes, respectively. Then we have

$$\sigma = \sigma_o \mathcal{F}(\sigma_o, t, M, T) \quad \text{for tension} \tag{4}$$

and

$$\tau = \tau_o \mathcal{b}(\tau_o, t, M, T) \quad \text{for shear,} \tag{5}$$

where σ and τ are the stresses at time t, σ_o and τ_o are the initially applied stresses, M represents the materials and specimen structure parameters, and T is the temperature. Again, we need to establish the relations between the two relaxation functions, $\mathcal{F}(\sigma_o, t, M, T)$ and $\mathcal{b}(\tau_o, t, M, T)$. Based on facts 1 and 2 in Section 3, together with the fact that part of the elastic strain is converted into plastic strain during stress relaxation, Eq. (4) can be rewritten as

$$2\tau = 2\tau_o \mathcal{F}(\sigma_o, t, M, T)$$

or

$$\tau = \tau_o \mathcal{F}(\sigma_o, t, M, T).$$

This means that relaxation functions $\mathcal{F}$ and $\mathcal{b}$ are same if σ_o is set equal to $2\tau_o$. Therefore, we have

$$\mathcal{b}(2\tau_o, t, M, T) \equiv \mathcal{F}(\sigma_o, t, M, T), \tag{6}$$

and it is concluded that the uniaxial tension stress-relaxation data can be applied to shear loaded cases.

5. Relaxation Test Data for 302 SS

Long duration stress relaxation tests were conducted for 302 SS wires of 0.05 in. diam. The stress levels varied from 0.5 to 0.75 of the F_{tu} value. The tests were performed in the Mechanics and Materials Technology Center (MMTC) at The Aerospace Corporation. The room used to conduct the tests was maintained at constant temperature (70°F ± 0.5°F) and constant humidity (60% ± 5%). Also, the tested wire specimens were the same length. Therefore, the relaxation function $\mathcal{F}(\sigma_o, t, M, T)$ for this case is independent of M and T.

From the uniaxial test data, the tension relaxation function was expressed as

$$\mathcal{F}(\sigma_o, t, M, T) = 1\text{-}S \log (t), \qquad (7)$$

where t is in hours. The S is expressed as a linear function of the applied initial stress, σ_o, i.e.,

$$S = S_o + \kappa\, \sigma_o.$$

Use of the test data $\sigma_o = 131$ ksi, $S = 0.0065$

$\sigma_o = 179$ ksi, $S = 0.0116$

gives $S_o = -0.0074$ and $\kappa = 0.000106$.

A higher order S vs σ_o relation can be easily obtained when stress relaxation at more stress levels is available.

Stress relaxation tests was also conducted on a V-band compression spring made of 302 SS circular wires. The dimensions of spring, wire, applied initial load, moment, and the load relaxation are listed as follows:

Spring diam = 0.778 in.
Wire diam = 0.07 in.
Initial load = 16.2 lb; final load = 15.86 lb.
Initial M_o = 16.2 x 0.778/2 = 6.3 in-lb.
Test time = 1000 hr (extrapolated).
Percentage of load relaxation = 2.1%.

6. Prediction Technique of Torque Relaxation for Compression Springs

We now are in a position to predict the torque relaxation in a compression spring by the use of Eq. (6) and to compare the prediction with the actual experimental observation. Consider a compression spring of circular cross-sectioned wires. We also designate the following symbols:

M = the applied torque equal to $PD/2$.
P = applied compression load.
D = Spring diam.
d = wire diam.

The shear stress in the wire is expressed as

$$\tau = (16PDr/\pi d^4)K, \tag{8}$$

with the maximum value as

$$\tau_{max} = (8PD/\pi d^3)K,$$

where

r = radial location from center of the wire where the shear stress is calculated.
K = a stress concentration factor equal to $(4C-1)/(4C-4) + 0.615/C$.
$C=D/d$.

To determine the torque relaxation in the spring, we use Eqs. (6), (7), and (8) in the following torque equation for the wire cross-section:

$$\tau/\tau_o = 1-(S_o + 2\kappa\tau_o)\log(t) \tag{9}$$

$$M_t = 2\pi \int_0^{d/2} \tau_o r^2 dr \, ,$$

which gives

$$M_t / M_o = 1 - S_o \log(t) - (128M_o/5\pi d^3)\kappa \log(t), \tag{10}$$

where

$M_o = \tau_{max}\, \pi d^3/16PD.$

Note that the stress concentration factor K was dropped in the Eq. (10) for simplicity. Since M_t/M_o is a ratio in which K drops out, the value of K does not affect Eq. (10).

A substitution of the S_o and κ values into Eq. (10) yields a M_t/M_o ratio of 0.974. In other words, the predicted load relaxation for this compression spring is 2.6%, which compares well with the 2.1% measured value. The difference is due to several possible reasons. These reasons include bilinear stress-strain and linear S vs σ_o assumptions used in the derivation. Another possible source of error is the ultimate tensile strength of the wire materials. For the 0.05 in. diam wire, the ultimate tensile strength is between 262 and 267 ksi. For the 0.07 in. diam wire, the ultimate tensile strength decreases to the 250-280 ksi range. This represents a 4% difference. A more accurate representation of the stress-strain curve will improve the accuracy. Also, Eq. (10) can be refined to include higher terms of σ_o when the relaxation function becomes nonlinear.

7. Determination of Residual Stresses

Residual stresses are often generated in both compression and torsion springs by presetting the springs. The residual stresses generate as a result of the plastic yielding of the spring wires, followed by an unloading of the spring. The residual stresses always act in the opposite direction to the operating stresses, thus increasing the range of the operating stress without inducing further plastic yielding.

The mathematical determination of the residual stresses in the compression and torsion springs needs to be treated differently from that in torsion springs, as described below.

7.1 Residual Stresses in a Compression Spring with a Circular Wire Cross section

Assume that part of the wire cross section is plastically yielded due to the application of an external torque M_t, and that the stress distribution in the wire is bilinear, as shown in Figure 2b. At a distance aR from the center of the wire, the shear stress is τ_o. Therefore, the stress τ as a function of r is expressed as

$$\tau = \tau_o r/(aR) \qquad 0 \le r \le aR \qquad (11a)$$

$$\tau = [(1 - \alpha) + \alpha r/(aR)]\, \tau_o \qquad aR \le r \le R. \qquad (11b)$$

The external M_t is then equal to the summation of two integrations, expressed as

$$M_t = \int_0^{aR} 2\pi r^2 \tau_o r / (aR) dr + \int_{aR}^{R} 2\pi r^2 [(1-\alpha) + \alpha r / (aR)] \tau_o dr \qquad (12a)$$

The result is

$$M_t = \pi \tau_o R^3 \, [a^3 / 2 + 2\,(1-\alpha)(1-a^3) / 3 + \alpha\,(1-a^4) / 2a]$$

or

$$M_t / M_e = [a^3 + 4\,(1-\alpha)(1-a^3) / 3 + \alpha\,(1-a^4) / a], \qquad (12b)$$

where $M_e = \pi\tau_o R^3/2$ is the torque with a maximum shear stress equal to τ_o at r = R. For 302 SS wire, the value of τ_o is 107.5 ksi. For a given value of M_t / M_e, the corresponding value of a can be solved algebraically. The shear stress distribution in the wire can be then determined using Eqs. (11a) and (11b).

In order to obtain the residual stress, the external torque M_t needs to be unloaded elastically. The stress distribution corresponding to this unloading is linear and is expressed as

$$\tau' = - 2\, M_t\, r/\pi\, R^4. \tag{13}$$

A combination of Eqs. (11a), (11b), and (13) gives the distribution of the shear stresses for any given M_t/M_e. Figure 3 depicts the residual stress distribution for 302 SS with an 0.05 in. wire diam and a M_t/M_e value of 2. It is seen that the maximum residual stress is about 24 ksi, which is approximately 22% of the elastic limit stress of 302 SS in shear.

7.2 Residual Stress Determination for a Torsion Spring with a Rectangular Wire Cross section

Assume the wire has a width b (in the direction parallel to the axis of the spring) and a depth of 2D (in the direction parallel to the radius of the spring). Again, assume the cross section is partly yielded plastically, due to the application of an external bending moment, M_b. The bilinear stress-strain curve is as shown in Figure 2a. The elastic stress, σ_o, is 215 ksi.

Similar to the distributions in the shear, the elastic and inelastic stress distributions in the cross section are expressed as

$$\sigma = \sigma_o\, x/(aD) \qquad 0 \le x \le aD \tag{14a}$$

$$\sigma = [(1 - \alpha) + \alpha\, x/(aD)]\, \sigma_o \qquad aD \le x \le D. \tag{14b}$$

The bending moment, M_b, is

$$M_b = 2\, \sigma_o\, bD^2 / 3\, [a^2 + 3\,(1 - \alpha)\,(1 - a^2) / 2 + (1 - a^3)\, \alpha / a]$$

or

$$M_b / M_{be} = [a^2 + 3\,(1 - \alpha)\,(1 - a^2) / 2 + (1 - a^3)\, \alpha / a], \tag{15}$$

where

$$M_{be} = 2\, \sigma_o\, bD^2 / 3.$$

For unloading elaastically, the stress distribution for the moment, M_b, is expressed as

$$\sigma_o' = - 3\, M_b\, x/(2bD^3). \tag{16}$$

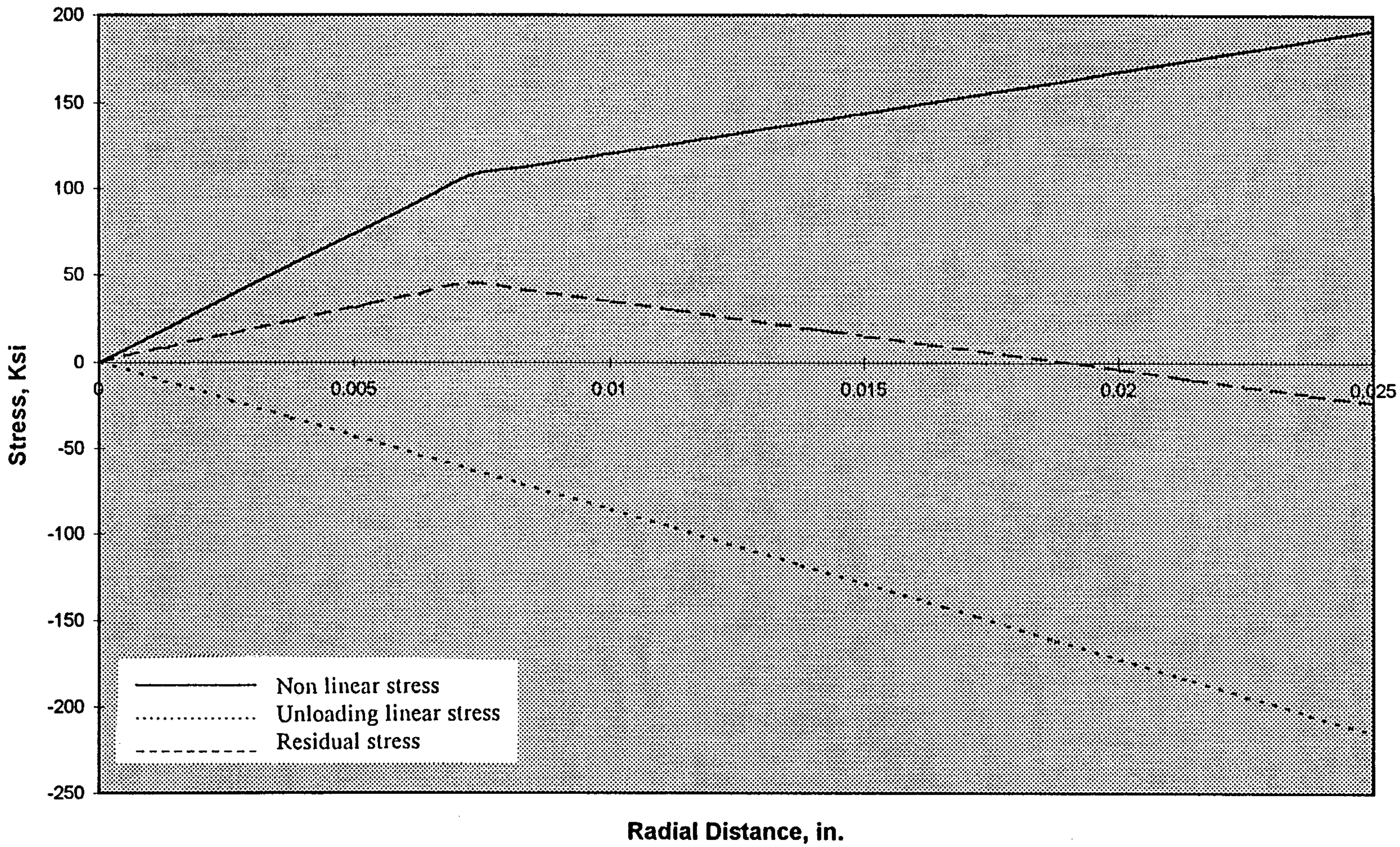

Figure 3. Typical nonlinear stress, unloading linear stress, and residual shear stress distributions in a 302 SS 0.05 in. diam wire.

A combination of Eqn. (14a), (14b), and (16) gives the residual stresses in the cross section. A case with M_b/M_{be} of 2 was worked out for b = D = 0.05 in. The residual stress distribution is depicted in Figure 4. A residual compressive stress of 43 ksi corresponding to 20% of the elastic limit stress is obtained.

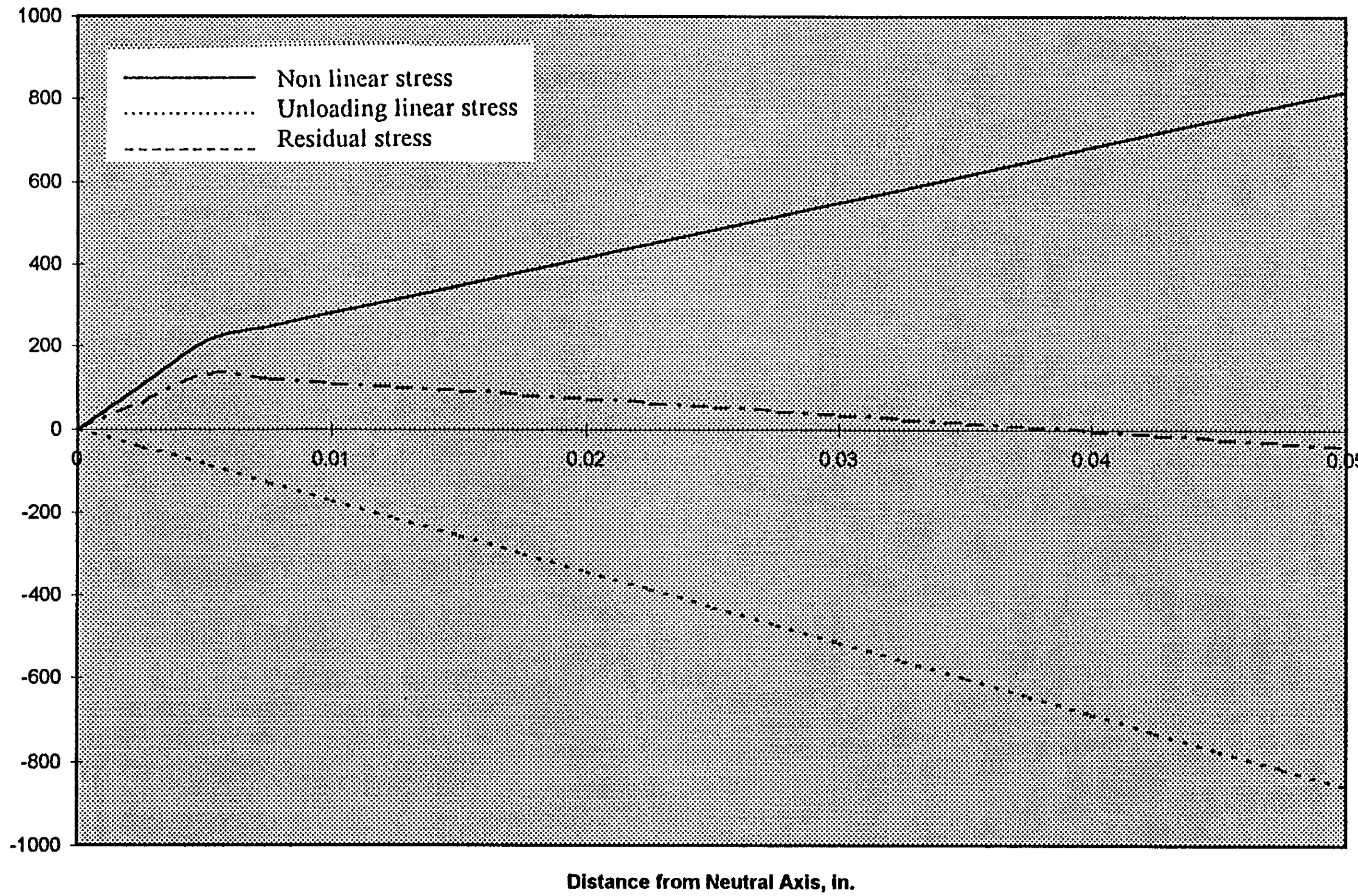

Figure 4. Typical nonlinear stress, unloading linear stress, and residual bending stress distributions in a 302 SS 0.05 in. square cross-sectioned wire.

8. Summary

An analytical technique was developed to predict the stress relaxation for compression and torsion springs. In this technique, the shear stress-strain curve is first constructed based on the uniaxial tension stress-strain curve. Next, an understanding is established that stress relaxation is a phenomenon in which part of the elastic strain responsible for the initial stress is replaced by plastic strain. The construction of a shear stress-strain curve is based on the following two facts:

1. Plastic strain is solely caused by shear strain.

2. Maximum shear stress is half of the tensile stress in a uniaxial tensile specimen.

It is concluded that the stress-relaxation function for a tension field can be easily converted into a stress-relaxation function for a shear stress field. An equation is finally derived to predict the torque ratio for 302 SS compression springs using this relaxation function.

The tensile stress-relaxation function for 302 SS wires that was experimentally determined by MMTC is successfully used to predict the torque reduction for a 302 SS V-band compression spring. The predicted 2.6% load reduction after 1000 hr compares well with the 2.1% load reduction obtained from tests. Although the derived equation is based on the linear dependency of initial stress, refinement can be made when more experimental data become available at more initial stress levels. However, only limited stress relaxation testing is currently available on the wire level. Therefore, testing on actual springs is greatly needed to validate the developed prediction technique.

Residual stress prediction methods for both compression and torsion springs are described. Examples presented here indicate that the residual stresses can be a significant portion of the elastic limit stress and are beneficial in actual satellite or launch operations.

TECHNOLOGY OPERATIONS

The Aerospace Corporation functions as an "architect-engineer" for national security programs, specializing in advanced military space systems. The Corporation's Technology Operations supports the effective and timely development and operation of national security systems through scientific research and the application of advanced technology. Vital to the success of the Corporation is the technical staff's wide-ranging expertise and its ability to stay abreast of new technological developments and program support issues associated with rapidly evolving space systems. Contributing capabilities are provided by these individual Technology Centers:

Electronics Technology Center: Microelectronics, VLSI reliability, failure analysis, solid-state device physics, compound semiconductors, radiation effects, infrared and CCD detector devices, Micro-Electro-Mechanical Systems (MEMS), and data storage and display technologies; lasers and electro-optics, solid state laser design, micro-optics, optical communications, and fiber optic sensors; atomic frequency standards, applied laser spectroscopy, laser chemistry, atmospheric propagation and beam control, LIDAR/LADAR remote sensing; solar cell and array testing and evaluation, battery electrochemistry, battery testing and evaluation.

Mechanics and Materials Technology Center: Evaluation and characterization of new materials: metals, alloys, ceramics, polymers and composites; development and analysis of advanced materials processing and deposition techniques; nondestructive evaluation, component failure analysis and reliability; fracture mechanics and stress corrosion; analysis and evaluation of materials at cryogenic and elevated temperatures; launch vehicle fluid mechanics, heat transfer and flight dynamics; aerothermodynamics; chemical and electric propulsion; environmental chemistry; combustion processes; spacecraft structural mechanics, space environment effects on materials, hardening and vulnerability assessment; contamination, thermal and structural control; lubrication and surface phenomena; microengineering technology and microinstrument development.

Space and Environment Technology Center: Magnetospheric, auroral and cosmic ray physics, wave-particle interactions, magnetospheric plasma waves; atmospheric and ionospheric physics, density and composition of the upper atmosphere, remote sensing using atmospheric radiation; solar physics, infrared astronomy, infrared signature analysis; effects of solar activity, magnetic storms and nuclear explosions on the earth's atmosphere, ionosphere and magnetosphere; effects of electromagnetic and particulate radiations on space systems; space instrumentation; propellant chemistry, chemical dynamics, environmental chemistry, trace detection; atmospheric chemical reactions, atmospheric optics, light scattering, state-specific chemical reactions and radiative signatures of missile plumes, and sensor out-of-field-of-view rejection.